Zhao *et al. Chem. Biol. Technol. Agric.* (2023) 10:135
https://doi.org/10.1186/s40538-023-00509-1

Chemical and Biological Technologies in Agriculture

RESEARCH

Open Access

Identification of physiological and metabolic networks involved in postharvest browning of cigar tobacco leaves

Gaokun Zhao[1†], Qing Zhang[2†], Guanghui Kong[1], Heng Yao[1], Yuping Wu[1], Bo Cai[3], Tao Liu[2*] and Guanghai Zhang[1*]

Abstract

The surface color of cigar tobacco leaves (CTLs) is largely determined by the browning response and is one of the most important quality traits affecting consumer preferences. The physiological changes and metabolic network of browning in CTLs after harvest have not been reported. We investigated the molecular mechanism of browning in CTLs by comparing the physiological characteristics and metabolites of CTLs browning at five postharvest periods. Phenotypic traits and browning-related enzyme activity data indicated that the browning reaction was most intense at approximately 12 d when polyphenol oxidase and peroxidase activities reached their maximum. Postharvest CTLs polyphenols, polyacids, and carbon and nitrogen compounds were rapidly degraded during the yellowing phase, and the biosynthesis rate of polyphenols and carotenoids was greater than the degradation rate during the browning phase. Metabolomic analysis discovered 2027 metabolites that were annotated mainly to lipids and lipid-like molecules, organic acids and their derivatives, and organic heterocyclic components. Hierarchical cluster analysis discovered glutamate, serine, threonine, ornithine, and arginine as the major amino acids involved in the browning reaction. KEGG pathway enrichment analysis indicated that the metabolic pathways with important effects on enzymatic browning were phenylpropanoid biosynthesis, flavonoid biosynthesis, isoquinoline alkaloid biosynthesis, phenylalanine metabolism, and linoleic acid metabolism. The metabolic pathway network was mined, and the main polyphenols involved in the browning reaction of CTLs were found to be cyanidin, rutin, caffeoylquinic acid, kaempferol, naringin, and neohesperidin. This study provides a reference for the browning physiology and metabolism network of postharvest CTLs.

Keywords Cigar tobacco leaf, Postharvest browning, Physiological change, Metabolic network

†Gaokun Zhao and Qing Zhang should be regarded as joint first authors.

*Correspondence:
Tao Liu
yantao618@126.com
Guanghai Zhang
zghzxf@126.com
Full list of author information is available at the end of the article

Graphical Abstract

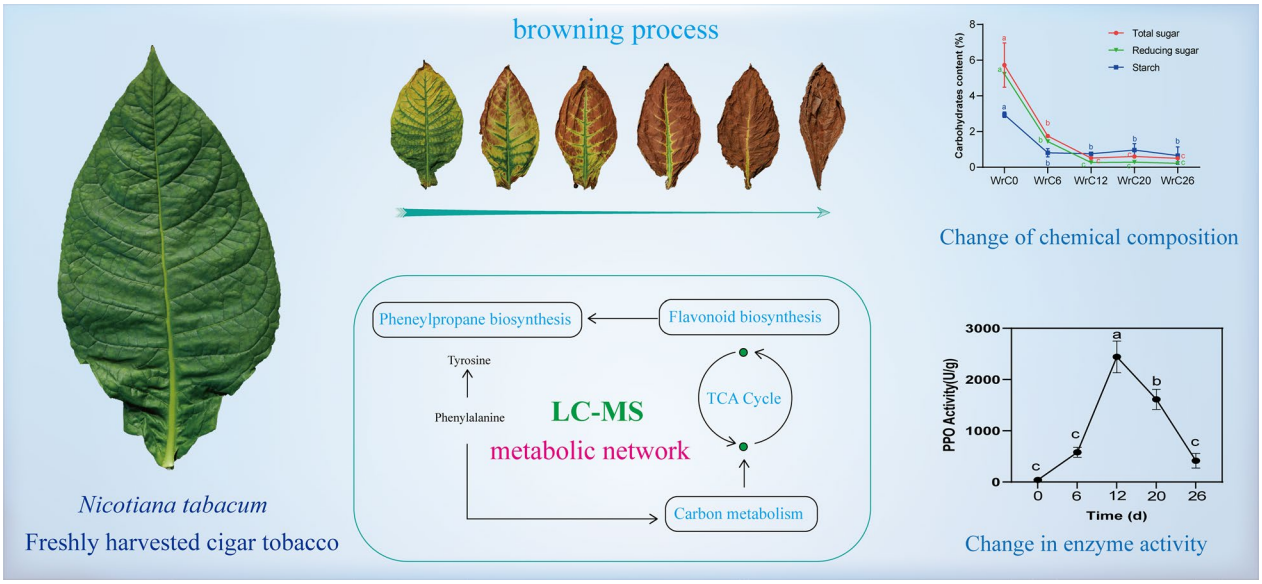

Introduction

The browning reaction is a phenomenon in which food products undergo a series of reactions to produce brown polymers during heating or long-term storage. Proper browning during the processing of substances, such as soy sauce, coffee, tobacco, black tea, and bread, helps to adjust the color and taste and develop a unique flavor [1–3]. However, the browning of fresh fruits and vegetables, such as apples, potatoes, and pineapples, after damage not only affects the sensory quality but also may reduce the nutritional value [4–6]. Cigar tobacco leaves harvested after maturation are left to dry for some time. Due to the browning process, the color gradually changes from green to brown or tawny over time [7, 8] and develops a unique flavor profile [9, 10]. However, Chen Y et al. noted that excessive browning reactions can lead to gray spots on tobacco leaves, which affect the value and industrial availability of tobacco leaves [1].

Browning reactions are generally classified into enzymatic browning and nonenzymatic browning according to the mechanism. Enzymatic browning is the oxidation of polyphenols to quinones by the action of polyphenol oxidase (PPO) and peroxidase (POD), followed by the formation of brown pigments by polymerization of these quinones and their derivatives [11]. Polyphenolic compounds are substrates for enzymatic browning, mainly including phenolic acids such as caffeic acid and ferulic acid, cyclohexanes such as quinic acid and shikimic acid, and coumarins such as hesperidin and scopoletin [12]. The content of polyphenols in CTLs was positively correlated with the quality, aroma, and taste of tobacco leaves, and the most important polyphenolic compounds within tobacco were chlorogenic acid, rutin, and scopoletin [12]. The previous studies showed that increasing the content of chlorogenic acid in eggplant flesh increased the susceptibility of eggplant flesh to browning [13]. Lu et al. found that flavonoids in mushrooms, including apigenin, lignan, kaempferol, and quercetin, promoted tyrosinase-induced browning in a model system and under aerobic conditions [14].

Metabolic enzymes are necessary for enzymatic browning when reactive oxygen species accumulate and a large number of free radicals with the participation of lipoxygenase (LOX) trigger membrane lipid peroxidation, disrupting the membrane structure and releasing metabolites from the cell. PPO and POD catalyze the oxidation of various substrates, including chlorogenic acid, ferulic acid, and *p*-hydroxycinnamic acid, to produce dark-colored substances [11]. Phenylalanine ammonia lyase (PAL) catalyzes the deamination reaction of phenylalanine to form polyphenols, providing a substrate supply. POD is capable of oxidizing not only chlorogenic acid and catechins but also several quercetin glycosides. However, POD is usually rarely involved in the enzymatic browning of fruits and vegetables after mechanical stress.

Non-enzymatic browning occurs when carbonyl compounds (reducing sugars, aldehydes, or ketones) and amino compounds (amino acids, peptides, or proteins)

are condensed during heating or prolonged storage, a reaction that does not involve enzymes. The reactions include Maillard reaction, caramelization, and ascorbic acid oxidation reactions [3, 15–18]. These reactions often occur in combination rather than independently. The type of amino acid in the Maillard reaction determines the resulting flavor and is the basis of the flavoring industry. Caramelization is the process of sugar oxidation and is widely used in cooking because of the nutty flavor and brown color it produces [19]. Heterocyclic compounds, such as furfural, furfuryl alcohol, pyridine, pyrrole, and furan formed by nonenzymatic reactions, are the main reasons for the strong aroma of CTLs.

It has been shown that a proper browning reaction has a positive effect on improving the quality of tobacco leaves [8, 12]. The browning mechanism of apples, pineapples, wheat seeds, potatoes, etc. has been explained, and enzymes and metabolites that affect browning have been searched for [2, 14, 20, 21]. However, the current studies mainly focus on the browning process of fruits and vegetables and their methods to inhibit browning, without elaborating on the browning response and metabolic network regulation mechanism of CTLs after harvesting, which is notably incomplete.

Untargeted metabolomics provides an "unbiased" view of the global metabolome with the ability to simultaneously identify and quantify a large number of endogenous metabolites [22]. Metabolomic analysis of postharvest CTLs helps to provide a comprehensive understanding of metabolite changes during the browning process [23]. In this study, we determined the physicochemical properties of CTLs during the air-curing process, analyzed the metabolites at different periods of air-curing using nontargeted metabolomics techniques, and revealed the changes and regulatory mechanisms of browning-related metabolites.

Materials and methods

Preparation of CTLs

Cigar tobacco (*Nicotiana tabacum*, var. Yunxue No.1) samples were collected in 2020 from the experimental field in Chengjiang County, Yunnan Province, China (Additional file 1: Table S1). The collected tobacco leaves were strung together, hung on bamboo poles, and placed in an air-curing room under natural conditions. Samples were randomly selected at 0, 6 d, 12 d, 20 d, and 26 d, with three replicates of each sample. Using the five-point sampling method, approximately 10 g of samples were cut between the branch veins of the tobacco leaves with sterilized scissors in centrifuge tubes, immediately snap-frozen in liquid nitrogen for 1 h, and then placed in a −80 °C refrigerator for freezing.

Enzyme activity determination

Phenylalanine ammonia lyase (PAL), polyphenol oxidase (PPO), peroxidase (POD), and lipoxygenase (LOX) activities were determined using SolarBio's microassay ELISA kits, utilizing approximately 0.1 g per sample, and kits were applied according to the manufacturer's instructions and assayed using an enzyme marker [13].

Chemical composition determination

The measurements of total sugars, reducing sugars, starch, total nitrogen, and alkaloids in tobacco were carried out using a continuous flow analysis system in accordance with tobacco industry standards (YC/T 159-2019, YC/T 216-2013, YC/T 161-2002, YC/T 468-2013). The content of polyacids was determined by gas chromatography according to the tobacco industry standard (YC/T 288-2009). The polyphenols and plasmatic pigments in tobacco were determined by high-performance liquid chromatography according to tobacco industry standards (YC/T 202-2006, YC/T 382-2010).

Nontargeted metabolomics analysis

The collected samples were ground to a powder with liquid nitrogen and then extracted with 80% aqueous methanol solution three times consecutively for each tobacco sample. An equal volume of samples from each experimental sample was mixed as quality control (QC) samples, and QC samples were disposed of and tested in the same way as analytical samples and measured every eight samples. A certain amount of supernatant was diluted with mass spectrometry grade water to 53% methanol and centrifuged at 15,000 g and 4 ℃ for 20 min, and the supernatant was collected and injected for LC–MS analysis [22, 24, 25]. LC–MS analyses were performed using a Vanquish UHPLC system (ThermoFisher, Germany) coupled with an Orbitrap Q Exactive™ HF mass spectrometer (Thermo Fisher, Germany). Samples were injected onto a Hypesil Goldcolumn (100×2.1 mm, 1.9 μm) using a 17-min linear gradient at a flow rate of 0.2 mL/min. The eluents for the positive polarity mode were eluent A (0.1% FA in Water) and eluent B (Methanol). The eluents for the negative polarity mode were eluent A (5 mM ammonium acetate, pH 9.0) and eluent B (Methanol).The solvent gradient was set as follows: 2% B, 1.5 min; 2–85% B, 3 min; 85–100% B, 10 min; 100–2% B, 10.1 min; 2% B, 12 min. Q Exactive™ HF mass spectrometer was operated in positive/negative polarity mode with spray voltage of 3.5 kV, capillary temperature of 320 ℃, sheath gas flow rate of 35 psi and aux gas flow rate of 10 L/min, S-lens RF level of 60, Aux gas heater temperature of 350 ℃.

Data processing

The raw data were processed using Compound Discoverer 3.1 (CD3.1, ThermoFisher) for simple screening of parameters such as retention time and mass-to-charge ratio for each metabolite and then setting retention time deviation of 0.2 min and mass deviation of 5 ppm for peak alignment of different samples to make identification more accurate, followed by setting mass deviation of 5 ppm, signal intensity deviation of 30%, signal-to-noise ratio of 3, minimum signal intensity, summed ions, and other information for peak extraction, while quantifying the peak area, then integrating the target ions, predicting the molecular formula by molecular ion peaks and fragment ions and comparing with mzCloud (https://www.mzcloud.org/), mzVault and Masslist databases, removing the background ions with blank samples, and normalizing the original quantification results to obtain the relative peak areas. Statistical analyses were performed using the statistical software R (R version R-3.4.3), Python (Python version 2.7.6), and CentOS (CentOS version 6.6). When the data were not normally distributed, compounds with a CV greater than 30% of the relative peak area in the QC samples were removed, and the metabolite identification and relative quantification results were obtained.

Statistical analysis

Enzyme-specific activity and chemical composition parameters were analyzed by one-way analysis of variance (ANOVA) using the IBM SPSS software (Version 25.0.0.2) and visualized by GraphPad Prim9 (Version 9.3.0). The KEGG database (https://www.genome.jp/kegg/pathway.html), HMDB (https://hmdb.ca/metabolites), and LIPIDMaps database (http://www.lipidmaps.org/) were used to identify metabolites for annotation [26]. The data were transformed using metaX [27] and subjected to principal component analysis (PCA) and partial least-squares discriminant analysis (PLS-DA) to obtain the VIP values for each metabolite. Statistical significance (P value) was calculated for each metabolite between the two groups based on a t test, and fold change (FC) values were calculated for the metabolites between the two groups. Metabolites with VIP > 1, $P < 0.05$, and FC ≥ 2 or FC ≤ 0.5 were defined as significantly different metabolites (DAMs). DAMs between different groups were mapped in KEGG by metabolic enrichment and pathway analysis based on database searches, and these DAMs were classified according to the pathways in which they were involved or the functions they performed. Volcano maps were generated using the R package ggplot2 in R (Version 2.15.3), hierarchical clustering heatmap were drawn using the R package ComplexHeatmap, and Pearson correlation analysis was performed using the R package Hmisc. Metabolic pathway network maps were drawn using Adobe Illustrator.

Results

Phenotypic characteristics of CTLs and changes in browning-related enzyme activities

Freshly harvested CTLs showed a dark green color, and the green color gradually faded from the leaf tip and leaf edge to the inside during air-curing, and the leaf color gradually turned yellow, and reddish brown until brownish brown with time, and the leaf shrank inwards and the flatness of leaf surface decreased. At 6 d, a slight brown change appeared in the apical part of the leaf; at 12 d, a large brown area appeared from outside to inside; at 16 d, almost all became brown except for the main veins and branch veins; and at 20 d and 35 d, all became brown except for the main leaf veins (Fig. 1A).

To explore the basic principle of brown color formation, we determined the period when the phenotype changed significantly, and then, the activities of PPO, POD, PAL, and LOX were quantified. The results showed that the specific activities of PPO and POD increased and then decreased during the air-curing process, reaching the highest value at 12 d. The specific activity of PAL showed an increasing trend, and the specific activity of LOX decreased at 6 d and increased at 12 d before maintaining a relatively stable level (Fig. 1B, C, D, E). We found that POD and LOX were very active during the air-curing process, indicating that these two enzymes played an important role. The activities of all four enzymes were relatively high at 12 d, especially PPO and POD, which reached their highest levels at this time. Combining the phenotypic traits and the changes in browning-related enzyme activities, we found that the browning reaction was more intense at approximately 12 d.

Changes in the chemical composition of CTLs

The intrinsic chemical composition is often an important determinant of color appearance. We quantitatively analyzed the dynamic changes in the chemical composition content of fresh tobacco leaves (WrC0), yellowing (WrC6), browning (WrC12), dry leaves (WrC20), and dry tendons (WrC26) after harvesting CTLs (Fig. 2). All compounds except polyacids and ions were rapidly degraded during the yellowing phase, especially the chlorophyll content. Among them, the chlorophyll b content decreased from 1316.50 ± 5.79 to 12.55 ± 0.06 μg/g, and the chlorophyll a content decreased from 1121.35 ± 0.84 to 75.91 ± 0.58 μg/g.

The content of polyphenols tended to decrease during the air-curing process, with the content of rutin increasing at WrC12 (Fig. 2A). The polyacids were relatively stable, with low contents of malonic acid and succinic acid

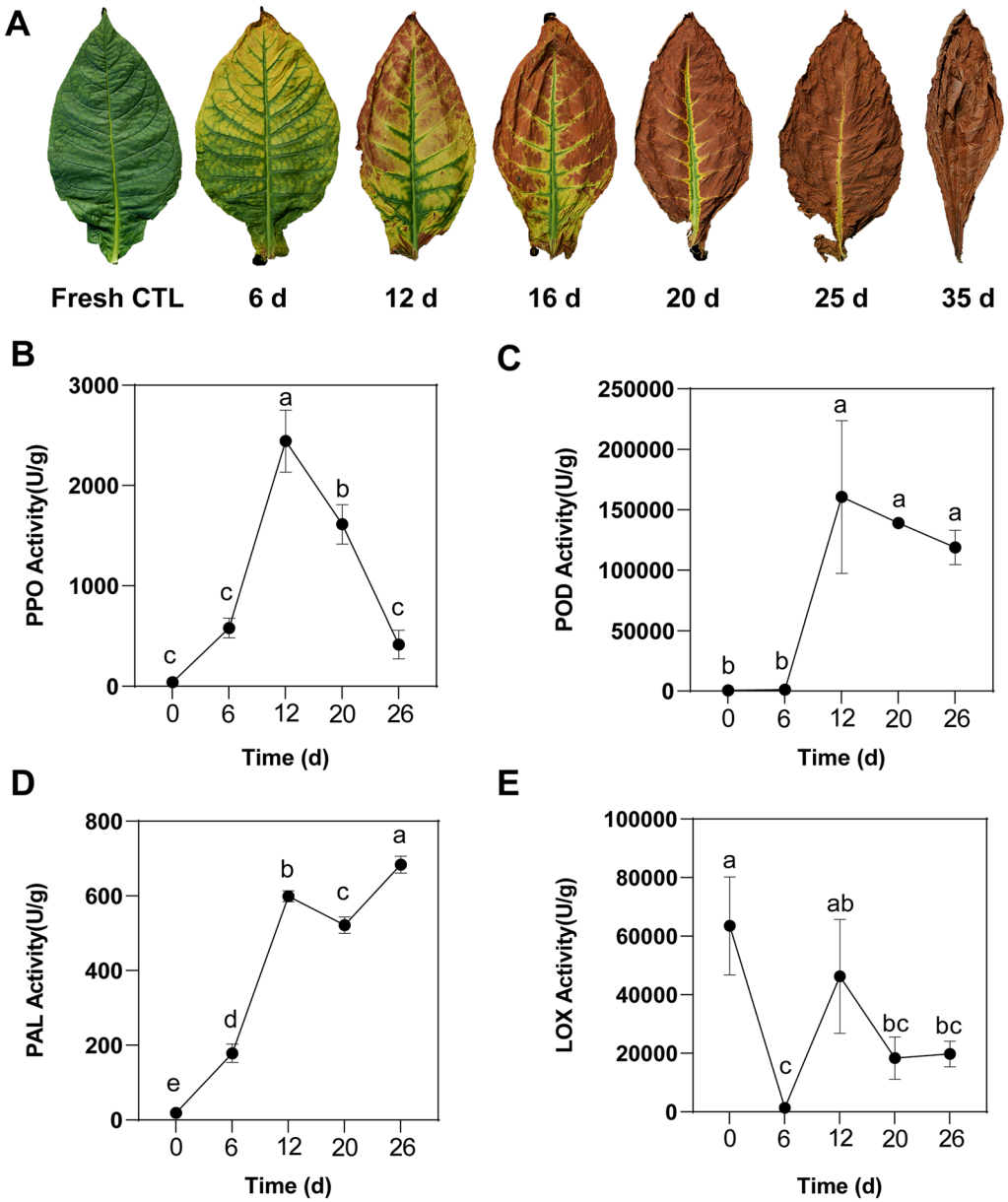

Fig. 1 Changes in phenotypic traits and browning-related enzyme activities of CTLs after harvesting. **A** Phenotypic changes in CTLs; **B** polyphenol oxidase (PPO) activity; **C** peroxidase (POD) activity; **D** phenylalamine ammonia lyase (PAL) activity; **E** lipoxygenase (LOX) activity. Data in the graphs are expressed as the mean ± SEM, and different letters indicate statistically significant differences of $p < 0.05$

(Fig. 2B). Carbon and nitrogen compounds decreased rapidly during the yellowing stage, and the content remained low after WrC12 (Fig. 2C, D). During the yellowing stage, the chlorophyll content declined rapidly and then remained at a low level. The carotenoid content declined slowly relative to chlorophyll (Fig. 2E). Potassium and chloride ions changed in opposite trends before the browning stage and in the same trend after the browning stage, and the potassium–chloride ratio was the minimum value of 1.34 ± 0.06 during the yellowing stage (Fig. 2F).

Untargeted metabolomics analysis of CTLs

The chemical composition analysis described above indicated that significant degradation of primary metabolites occurred during the air-curing process. Therefore, to fully characterize the metabolic profile of the browning process and to class key differential

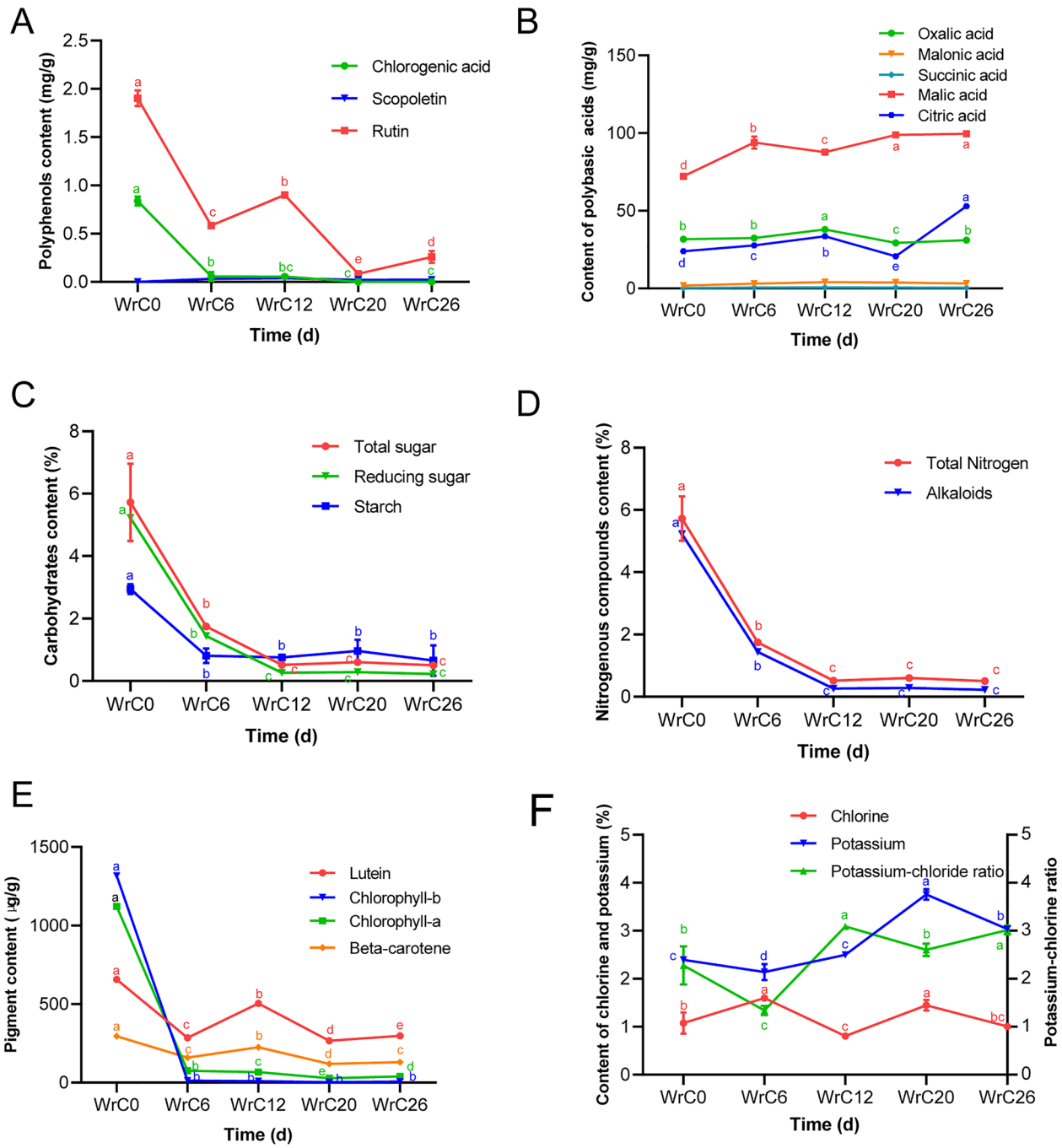

Fig. 2 Changes in the content of polyphenols (**A**), polyacids (**B**), carbohydrates (**C**), nitrogenous compounds (**D**), plastid pigments (**E**), and potassium ions and chloride ions (**F**) during the air-curing of CTLs. Data in the graphs are expressed as the mean ± SEM, and different letters indicate statistically significant differences of $p < 0.05$

metabolites, untargeted metabolomics was applied for analysis. A total of 2027 metabolites were discovered in the 27 samples in this project, 995 metabolites were annotated by HMDB, 605 metabolites by KEGG, and 214 metabolites by LIPIDMaps. Based on the relative quantitative values of metabolites to calculate the Pearson correlation coefficients between QC samples, the R2 > 98% for 8 QC samples indicated good stability of the whole assay process and high data quality (Additional file 1: Fig. S1).

PCA can be used to observe the overall metabolite differences between groups of samples, as well as the magnitude of variation between samples within groups.

The results showed that the confidence intervals of the three biological replicate samples within the group were all within 95% (Fig. 3), indicating good reproducibility within the group. In addition, the metabolites of the samples varied significantly among different groups. Among them, metabolic characteristics were close between the WrC12, WrC20, and WrC26 samples, and the chemical differences between WrC0 and WrC6 and these three were greater. This indicates that the changes in metabolites in the air-curing stage mainly occurred in the yellowing and browning stages, and the metabolites of the WrC20 and WrC26 samples were less changed.

Comparisons were made between two sample groups in different periods by the OPLS-DA method. R^2Y indicates the explanatory rate of the model, Q^2Y is used to evaluate the predictive ability of the OPLS-DA model, and $R^2Y > Q^2Y$ indicates a well-established model. According to the cross-validation, $R^2Y > 0.98$ and $R^2Y > Q^2Y$ for WrC0 vs. WrC6, WrC6 vs. WrC12, WrC12 vs. WrC20 and WrC20 vs. WrC26 indicated that the model was well established (Additional file 1: Table S2).

Analysis of differential metabolites in different periods of CTLs

By analyzing the change process of metabolites during the air-curing process of CTLs, a total of 824 DAMs were identified in the WrC0 vs WrC6 group, of which 194 were significantly down-regulated and 630 were significantly up-regulated (Additional file 1: Fig. S3A); 564 DAMs were identified in the WrC6 vs. WrC12 group, of which 356 were significantly down-regulated and 208 were significantly up-regulated (Additional file 1: Fig. S3B). A total of 141 DAMs were identified in the WrC12 vs. WrC20 group, of which 75 were significantly down-regulated and 66 were significantly up-regulated (Additional file 1: Fig. S3C), and a total of 383 DAMs were identified in the WrC20 vs. WrC26 group, of which 307 were significantly down-regulated and 76 were significantly up-regulated (Additional file 1: Fig. S3D). Based on HMDB superclasses, we classified and counted DAMs and found that the types of DAMs were basically the same in different groups, but the contents were significantly different. The WrC0 vs. WrC6 group and WrC6 vs. WrC12 group had the highest contents of lipids and lipid-like molecules (15.66% and 12.06%), the WrC12 vs. WrC20 group had the highest contents of organic acids and derivatives (17.02%), and the WrC20 vs. WrC26 group had the highest content of organic heterocyclic components (9.40%) (Additional file 1: Fig. S3E, F, G, H). The results indicated that lipid and lipid-like molecules, organic acids and derivatives, and organic heterocyclic fractions played an important role in the air-curing process.

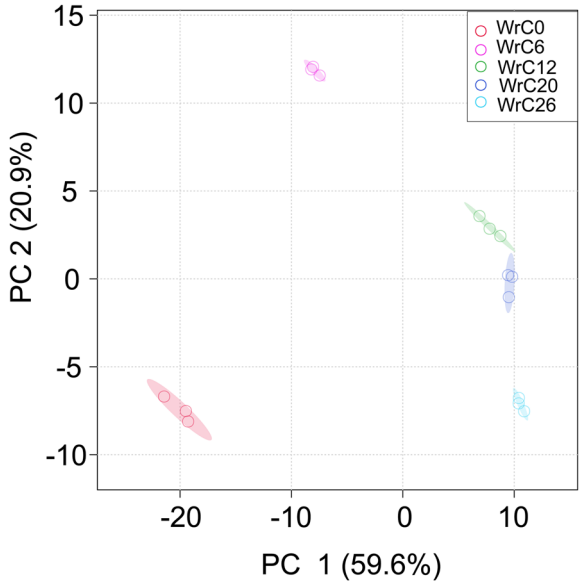

Fig. 3 Plot of principal component analysis scores during the browning of CTLs

To provide a clearer response to the dynamics of DAMs during air-curing, hierarchical clustering heatmaps were used to show DAMs that may be associated with browning. Amino acids and polyphenols were enriched mainly in fresh tobacco leaves, while derivatives of amino acids and phenols were mainly aggregated during air-curing. Formic acid and methyl ester polyphenolic substances were mainly enriched in fresh tobacco leaves, while phenolics, salicylic acid, butyric acid, and berberine were mainly enriched in WrC26 (Fig. 4A). The organic heterocyclic compounds in fresh tobacco leaves were mainly tryptamines, nicotine, and nicotinic acid substances, and WrC26 was mainly enriched in vitamin B3, L-5-hydroxytryptophan, and acids (Fig. 4B). The types of amino acids enriched in CTLs differed at different air-curing periods. Among them, fresh tobacco leaves were mainly enriched in L-aspartic acid, methionine, proline, serine, L-lysine, L-threonine, and L-cysteine; proline, threonine, valine, and asparagine were enriched in WrC6; WrC12 was mainly enriched in L-phenylalanine, glutamine, L-histidine, and glycine; and 4-hydroxyproline, D-proline, and arginine in the WrC26 period succinic acid were more abundant (Fig. 4C). Ferulic acid, vanillic acid, naringenin, and quercetin were enriched at WrC0, and naringenin, kaempferol, cinnamic acid, scopoletin, and rutin were enriched at WrC12 (Fig. 4D).

To better assess the metabolite differences and metabolic pathways involved in CTLs during air-curing, these

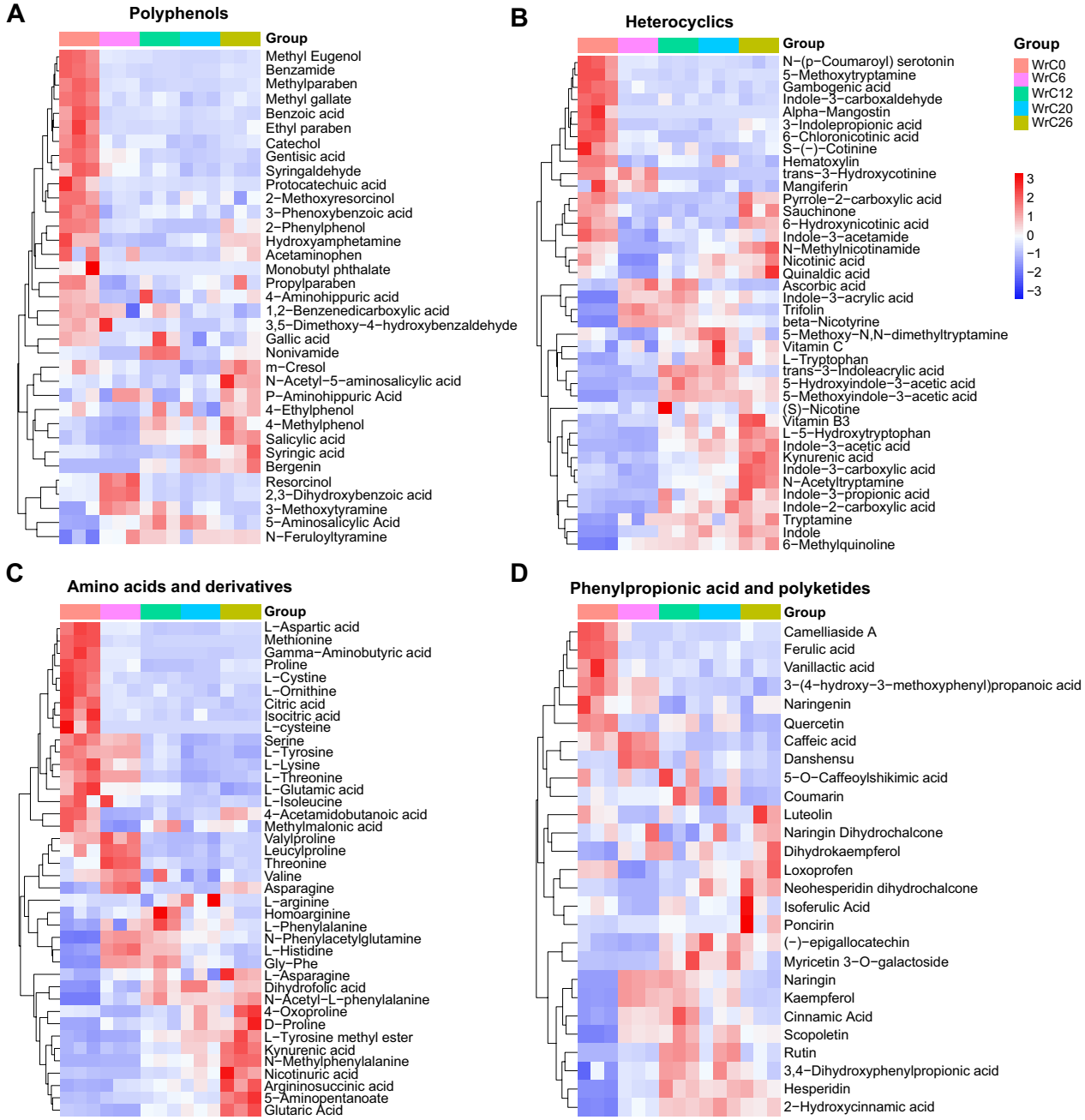

Fig. 4 Hierarchical clustering heatmap of differential polyphenols (**A**), heterocyclic compounds (**B**), amino acids and derivatives (**C**), phenylpropanoids, and polyketides (**D**)

metabolites and major metabolic pathways were annotated by KEGG analysis. The results showed that DAMs were mainly enriched in the pathways of arginine biosynthesis, aminoacyl tRNA biosynthesis, histidine metabolism, purine metabolism, phenylalanine metabolism, and pyrimidine metabolism. The important pathways affecting DAMs in the air-curing process were mainly phenylpropanoid biosynthesis, alanine, aspartate, and glutamate metabolism, tryptophan metabolism, flavonoid biosynthesis, isoquinoline alkaloid biosynthesis, phenylalanine metabolism, and linoleic acid metabolism (Fig. 5).

Discussion

CTLs brown during the air-curing process, and since the degree of browning reaction determines the appearance quality and inner quality of CTLs, it is important to

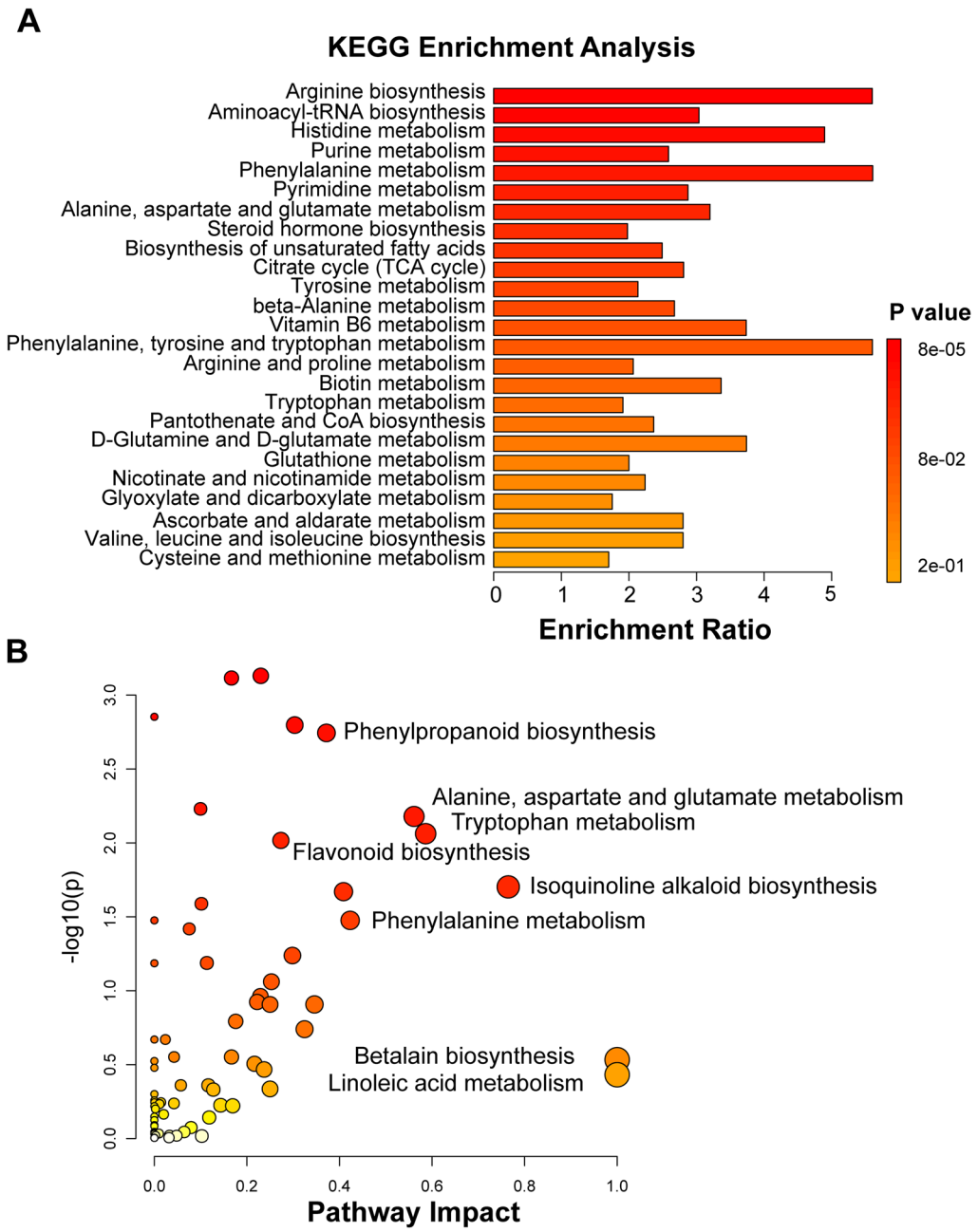

Fig. 5 KEGG enrichment analysis of DAM plots (**A**) and pathway impact plots (**B**). The color of the points represents the p-value, from white to red, the p-value is from big to small, the size of the points represents the pathway impact value, and the bigger the points, the bigger the impact value

understand the browning reaction during the air-curing process of CTLs [15, 17, 28–31].

Enzymatic browning occurs with the involvement of multiple enzymes. A large accumulation of ROS triggers membrane lipid peroxidation disrupts membrane structure, and stimulates membrane lipid catabolism under the action of LOX. In addition, oxidation of unsaturated fatty acids disrupts the fluidity of the cell membrane [13]. PAL is a key enzyme in the metabolism of phenylpropane and is involved in the synthesis of polyphenols. Enzymatic browning is a process in which phenolic substrates are catalyzed to form quinones with the participation of PPO and POD, and the polymerized quinones rapidly turn into dark pigments. The changes in the activities of POD, PAL, PPO, and LOX were analyzed. Freshly harvested CTLs immediately exhibited strong LOX activity,

which caused a decrease in cell membrane integrity and increased permeability, resulting in a large amount of metabolite efflux. Phenylalanine metabolism was vigorous at higher PAL activity, and polyphenols gradually accumulated. Enzymatic browning reaction of polyphenols took place with the participation of PPO and POD to form dark brown substances, resulting in the gradual turning of leaves into brown color from outside to inside. Unsaturated fatty acids, such as linoleic acid, were also involved in the oxidation process (Fig. 5). The strong activities of POD, PAL, PPO, and LOX during the browning stage indicated that a large number of polyphenolic substrates were synthesized at this time, cell membrane permeability continued to increase, and substrates were continuously oxidized, which was the most active period of the enzymatic browning reaction. Then, PPO activity decreased, and the enzymatic browning reaction gradually weakened. However, the activities of POD and PAL did not decrease significantly after the browning period, and the oxidation reaction and the accumulation of polyphenols continued to occur in the late air-curing period.

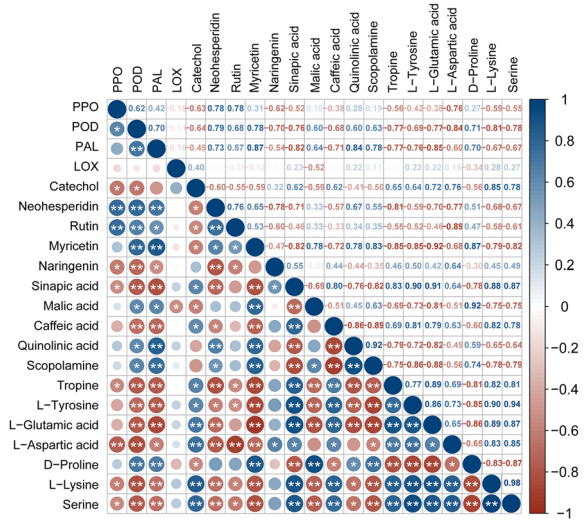

Fig. 6 Spearman correlation matrix between browning-related enzymes and metabolites. Blue indicates a positive correlation, red indicates a negative correlation, circle size indicates the strength of the correlation, and numbers indicate correlation coefficient values. * and ** indicate significant and highly significant differences ($p < 0.05$ and $p < 0.01$), respectively

The most important substrate for browning is polyphenols, and the synthesis of polyphenolic compounds originates from the metabolism of phenylalanine and tyrosine. PAL is the key enzyme involved in the metabolism of phenylalanine [32, 33]. Anthocyanin accumulation was correlated with PAL activity (Fig. 6), and most of the cyanidin had a bright color, suggesting that PAL activity may have an important effect on the color appearance of CTLs. The polyphenols mainly involved in synthesis and influencing enzymatic browning during the browning phase were caffeoylquinic acid, caffeic acid, quinic acid derivatives, etc. The PAL activity remained active in the middle and late stages of air-curing when the main polyphenol synthesized was scopoletin (Fig. 7). The tobacco phenylalanine metabolites benzyl benzoate

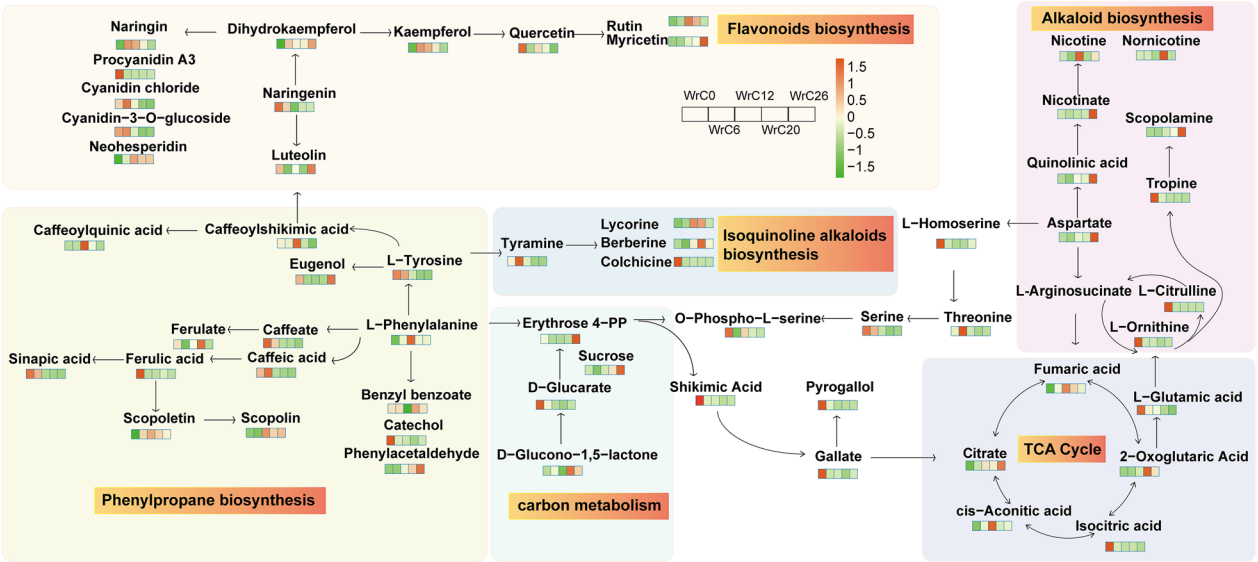

Fig. 7 Metabolic pathways of the main metabolites at different periods of air-curing. The bars show from left to right the metabolite content in WrC0, WrC6, WrC12, WrC20, and WrC26. The values represented by the colors are the quantitative results of the metabolites obtained based on the total peak area quantification and normalization

and phenylacetaldehyde were enriched in the late air-curing period, and benzyl benzoate and phenylacetaldehyde were among the more abundant aroma components in tobacco. The results indicated that polyphenols were mainly involved in the browning reaction in the middle repair-curing period, while the accumulation of polyphenols in the middle and late air-curing periods provided aromatic qualities.

Aspartic acid, proline, malic acid, and sugars lead to a Maillard reaction [34–37], giving tobacco a dark brown color, and some reaction products give it a distinctive aroma [38, 39]. We know that the metabolic enzymes of roasted tobacco are rapidly inactivated under high-temperature roasting, making the sugar and starch contents higher [40]. In contrast, CTLs underwent a mild air-curing process, and the sugar and starch contents were maintained at low levels (Fig. 2C). Glucose was mainly enriched in fresh tobacco leaves, while sucrose was mainly enriched in the dry tendon phase (Fig. 7). Reducing sugars such as glucose can themselves undergo caramelization reactions, as well as Maillard reactions. The degradation of sugars is associated with the Maillard reaction of the nonenzymatic browning process [18].

Free amino acids are precursors of nicotine and polyphenols and are key to nonenzymatic browning. The amino acid metabolic pathways that have an important impact on the air-curing process are alanine, aspartate, and glutamate metabolism and tryptophan metabolism (Fig. 6). Heterocyclic compounds, such as pyrroles, pyridines, and furans, tend to have unique aromas [9]. Among them, proline is a precursor of pyrrole, and tryptophan is a precursor of indole. Ornithine, citrulline, serine, and glutamic acid are mainly enriched in fresh tobacco leaves and then degraded through amino acid metabolic pathways to participate in the formation process of various aroma substances (Figs. 4, 7). Phenylalanine is the key to the biosynthesis of polyphenols and influences the metabolic process of carbohydrates. Aspartic acid controls the biosynthetic process of alkaloids. The degradation of tyrosine is key to the biosynthesis of flavonoids and flavonoids, producing cyanidin, such as kaempferol and cyanidin (Fig. 7). Among them, cyanidin were mainly enriched in fresh tobacco leaves and the yellowing stage, and rutin, caffeoylquinic acid, kaempferol, naringenin, and neohesperidin were mainly enriched in the yellowing and browning stages. The results showed that the bright color of the yellowing stage was not only derived from lutein and β-carotene but also related to cyanidin and flavonoids.

Endogenous anti-browning metabolites are also present within CTLs to prevent excessive browning. Carboxylic acids have been reported to have metal-chelating or pH-lowering effects, thus inhibiting browning. Tartaric acid, malonic acid, and oxalic acid have strong inhibitory effects on apple slice browning. Citric acid has been widely used as an anti-browning compound in the food industry [6]. It has been shown that lycopene can prevent enzymatic browning of fresh-cut apples [41]. The organic acids affecting browning in the repair-curing period were mainly isocitric acid and cis-aconitate, while lycopene, citric acid, fumaric acid, and 2-oxoglutaric acid mainly regulated the browning reaction in the middle and late air-curing periods (Fig. 7), and these carboxylic acids inhibited the excessive enzymatic browning reaction through negative regulation. Regulating the degree of browning within a reasonable range is important for controlling the intrinsic quality and sensory quality of tobacco leaves.

Conclusion

The browning reaction of CTLs during the air-curing process affects the quality of cigars. However, most relevant studies have focused on the browning of fruits and vegetables. To investigate the mechanisms associated with plant leaf browning, we performed physiological analyses and metabolomic approaches to systematically compare the changes in metabolic pathways during air-curing. The results showed that the membrane lipid permeability of freshly harvested CTLs increased rapidly, polyphenols accumulated gradually, and enzymatic browning began to occur with the participation of PPO and POD. The enzymatic browning reaction gradually increased in the middle of the repair-curing period and then decreased. Polyphenols were mainly involved in the browning reaction in the first and middle stages of air-curing, while they accumulated in the middle and late stages of air-curing to provide aromatic quality. Glutamic acid, serine, threonine, ornithine, and arginine were the key amino acids for nonenzymatic browning. Browning reaction inhibitors, such as isocitric acid, cis-aconitic acid, lycopene, and citric acid, regulate browning at stable levels through content changes.

Supplementary Information

The online version contains supplementary material available at https://doi.org/10.1186/s40538-023-00509-1.

Additional file 1: Figure S1. Pearson correlation coefficient plot for QC samples. **Figure S2.** Plot of the scores generated by the OPLS-DA model for different periods of the drying system. **Figure S3.** Volcano and pie charts of differential metabolites. **Table S1.** Sample Collection. **Table S2.** Explanatory and predictive power of the OPLS-DA model between different sample groups.

Author contributions

QZ: writing original draft. GZ: investigation. GK: conducted experiments and funding acquisition. HY: data curation. BC: methodology. YW: supervision. TL:

review and editing. GZ: designed experiment, conceptualization, review, and editing.

Funding
This research was funded by the China Tobacco Monopoly Bureau Grants (110 202103018/2022530000241002), Yunnan Provincial Tobacco Monopoly Bureau Grants (2020530000241001 and 2023530000241001), and Research and application of personalized cigarette products (2023CP02).

Availability of data and materials
The data underlying this paper will be shared on reasonable request to the corresponding author.

Declarations

Ethics approval and consent to participate
Not applicable.

Consent for publication
This research has been confirmed for publication in the journal.

Competing interests
The authors have no competing interests.

Author details
[1]Yunnan Academy of Tobacco Agricultural Sciences, Kunming 650021, Yunnan, China. [2]College of Agriculture and Biotechnology, Yunnan Agricultural University, Kunming 650201, Yunnan, China. [3]Technical Center of Yunnan Zhongyan Industry Co., Ltd, Kunming 650305, Yunnan, China.

Received: 12 September 2023 Accepted: 18 November 2023
Published online: 23 November 2023

References

1. Chen Y, Zhou J, Ren K, Zou C, Liu J, Yao G, He J, Zhao G, Huang W, Hu B, Chen Y, Xiong K, Jin Y. Effects of enzymatic browning reaction on the usability of tobacco leaves and identification of components of reaction products. Sci Rep. 2019;9:17850. https://doi.org/10.1038/s41598-019-54360-2.
2. Bork LV, Rohn S, Kanzler C. Characterization of colorants formed by non-enzymatic browning reactions of hydroxycinnamic acid derivatives. Molecules. 2022. https://doi.org/10.3390/molecules27217564.
3. Murata M. Browning and pigmentation in food through the Maillard reaction. Glycoconj J. 2021;38:283–92. https://doi.org/10.1007/s10719-020-09943-x.
4. Moon KM, Kwon EB, Lee B, Kim CY. Recent trends in controlling the enzymatic browning of fruit and vegetable products. Molecules. 2020. https://doi.org/10.3390/molecules25122754.
5. Li Q, Xu K, Wang S, Li M, Jiang Y, Liang X, Niu J, Wang C. Enzymatic browning in wheat kernels produces symptom of black point caused by Bipolaris sorokiniana. Front Microbiol. 2020;11:526266. https://doi.org/10.3389/fmicb.2020.526266.
6. Nicolas JJ, Richard-Forget FC, Goupy PM, Amiot MJ, Aubert SY. Enzymatic browning reactions in apple and apple products. Crit Rev Food Sci Nutr. 1994;34:109–57. https://doi.org/10.1080/10408399409527653.
7. Wu S, Guo Y, Adil MF, Sehar S, Cai B, Xiang Z, Tu Y, Zhao D, Shamsi IH. Comparative proteomic analysis by iTRAQ reveals that plastid pigment metabolism contributes to leaf color changes in tobacco (*Nicotiana tabacum*) during curing. Int J Mol Sci. 2020. https://doi.org/10.3390/ijms21072394.
8. Li N, Yu J, Yang J, Wang S, Yu L, Xu F, Yang C. Metabolomic analysis reveals key metabolites alleviating green spots under exogenous sucrose spraying in air-curing cigar tobacco leaves. Sci Rep. 2023;13:1311. https://doi.org/10.1038/s41598-023-27968-8.
9. Liu A, Yuan K, Xu H, Zhang Y, Tian J, Li Q, Zhu W, Ye H. Proteomic and metabolomic revealed differences in the distribution and synthesis mechanism of aroma precursors in Yunyan 87 tobacco leaf, stem, and root at the seedling stage. ACS Omega. 2022;7:33295–306. https://doi.org/10.1021/acsomega.2c03877.
10. Qin G, Zhao G, Ouyang C, Liu J. Aroma components of tobacco powder from different producing areas based on gas chromatography ion mobility spectrometry. Open Chem. 2021;19:442–50. https://doi.org/10.1515/chem-2020-0116.
11. Jw H. Treatment of tobacco to reduce polyphenol content. Atlanta, United States: Research corp; 1971.
12. Williamson RE, Gwynn GR. Variation of polyphenols in flue-cured tobacco cultivars attributed to location, stalk position, and year 1. Crop Sci. 1982;22:144–6.
13. Liu X, Xiao K, Zhang A, Zhu W, Zhang H, Tan F, Huang Q, Wu X, Zha D. Metabolomic analysis, combined with enzymatic and transcriptome assays, to reveal the browning resistance mechanism of fresh-cut eggplant. 2022. Foods. https://doi.org/10.3390/foods11081174.
14. Lu Y, Xu Y, Song MT, Qian LL, Liu XL, Gao RY, Han RM, Skibsted LH, Zhang JP. Promotion effects of flavonoids on browning induced by enzymatic oxidation of tyrosinase: structure-activity relationship. RSC Adv. 2021;11:13769–79. https://doi.org/10.1039/d1ra01369f.
15. Wu Z, Weeks WW, Long RC. Contribution of neutral volatiles to flavor intensity of tobacco during smoking. J Agric Food Chem. 1992;40:1917–21.
16. Sanz-Barrio R, Corral-Martinez P, Ancin M, Segui-Simarro JM, Farran I. Overexpression of plastidial thioredoxin f leads to enhanced starch accumulation in tobacco leaves. Plant Biotechnol J. 2013;11:618–27. https://doi.org/10.1111/pbi.12052.
17. Banožić M, Jokić S, Ačkar Đ, Blažić M, Šubarić D. Carbohydrates-key players in tobacco aroma formation and quality determination. Molecules. 2020. https://doi.org/10.3390/molecules25071734.
18. Luo Y, Zhang J, Ho C-T, Li S. Management of Maillard reaction-derived reactive carbonyl species and advanced glycation end products by tea and tea polyphenols. Food Sci Hum Wellness. 2022;11:557–67. https://doi.org/10.1016/j.fshw.2021.12.012.
19. Şen D, Gökmen V. Kinetic modeling of Maillard and caramelization reactions in sucrose-rich and low moisture foods applied for roasted nuts and seeds. Food Chem. 2022;395:133583. https://doi.org/10.1016/j.foodchem.2022.133583.
20. Dong T, Cao Y, Jiang CZ, Li G, Liu P, Liu S, Wang Q. Cysteine protease inhibitors reduce enzymatic browning of potato by lowering the accumulation of free amino acids. J Agric Food Chem. 2020;68:2467–76. https://doi.org/10.1021/acs.jafc.9b07541.
21. Ackah S, Xue S, Osei R, Kweku-Amagloh F, Zong Y, Prusky D, Bi Y. Chitosan treatment promotes wound healing of apple by eliciting phenylpropanoid pathway and enzymatic browning of wounds. Front Microbiol. 2022;13:828914. https://doi.org/10.3389/fmicb.2022.828914.
22. Want EJ, Masson P, Michopoulos F, Wilson ID, Theodoridis G, Plumb RS, Shockcor J, Loftus N, Holmes E, Nicholson JK. Global metabolic profiling of animal and human tissues via UPLC-MS. Nat Protoc. 2013;8:17–32. https://doi.org/10.1038/nprot.2012.135.
23. Jia-Xi L, Chun-Xia Z, Ying H, Meng-Han Z, Ya-Nan W, Yue-Xin Q, Jing Y, Wen-Zhi Y, Miao-Miao J, De-An G. Application of multiple chemical and biological approaches for quality assessment of *Carthamus tinctorius* L. (safflower) by determining both the primary and secondary metabolites. Phytomedicine. 2019;58:152826. https://doi.org/10.1016/j.phymed.2019.152826.
24. Wu X, Zhu R, Ren Z, Wang K, Mou D, Wei W, Miao M. Separation and identification of 5 glycosidic flavor precursors in tobacco by ultra performance liquid chromatography-electrospray ionization tandem mass spectrometry. Se Pu. 2009;27:820–4.
25. Li Y, Lin Q, Pang T, Shi J. Determination of 12 flavonoids in tobacco leaves using ultra-high performance liquid chromatography-tandem mass spectrometry. Se Pu. 2015;33:746–52. https://doi.org/10.3724/sp.j.1123.2015.03001.
26. Kanehisa M, Goto S. KEGG: kyoto encyclopedia of genes and genomes. Nucleic Acids Res. 2000;28:27–30. https://doi.org/10.1093/nar/28.1.27.
27. Wen B, Mei Z, Zeng C, Liu S. metaX: a flexible and comprehensive software for processing metabolomics data. BMC Bioinform. 2017;18:183. https://doi.org/10.1186/s12859-017-1579-y.

28. Gao J, Qin X, Tan Z, Li M. Influence of main chemical components on smoking quality of flue-cured tobacco. Shan Di Nong Ye Sheng Wu Xue Bao. 2004;23:497–501.
29. Talhout R, Opperhuizen A, van Amsterdam JGC. Sugars as tobacco ingredient: effects on mainstream smoke composition. Food Chem Toxicol. 2006;44:1789–98. https://doi.org/10.1016/j.fct.2006.06.016.
30. Sun W, Zhou Z, Li Y, Xu Z, Xia W, Zhong F. Differentiation of flue-cured tobacco leaves in different positions based on neutral volatiles with principal component analysis (PCA). Eur Food Res Technol. 2012;235:745–52. https://doi.org/10.1007/s00217-012-1799-3.
31. Hu Z, Pan Z, Yang L, Wang K, Yang P, Xu Z, Yu H. Metabolomics analysis provides new insights into the medicinal value of flavonoids in tobacco leaves. Mol Omics. 2021;17:620–9. https://doi.org/10.1039/d1mo00092f.
32. Tsao R. Chemistry and biochemistry of dietary polyphenols. Nutrients. 2010;2:1231–46. https://doi.org/10.3390/nu2121231.
33. Walter MH, Strack D. Carotenoids and their cleavage products: biosynthesis and functions. Nat Prod Rep. 2011;28:663–92. https://doi.org/10.1039/c0np00036a.
34. Zhou X, Xiao Y, Meng X, Liu B. Full inhibition of Whangkeumbae pear polyphenol oxidase enzymatic browning reaction by l-cysteine. Food Chem. 2018;266:1–8. https://doi.org/10.1016/j.foodchem.2018.05.086.
35. Lu S, Cui H, Zhan H, Hayat K, Jia C, Hussain S, Tahir MU, Zhang X, Ho CT. Timely addition of glutathione for its interaction with deoxypentosone to inhibit the aqueous maillard reaction and browning of glycylglycine-arabinose system. J Agric Food Chem. 2019;67:6585–93. https://doi.org/10.1021/acs.jafc.9b02053.
36. Nakamura M, Mikami Y, Noda K, Murata M. Browning of Maillard reaction systems containing xylose and 4-hydroxy-5-methyl-3(2H)-furanone. Biosci Biotechnol Biochem. 2021;85:401–10. https://doi.org/10.1093/bbb/zbaa019.
37. Zhai Y, Cui H, Zhang Q, Hayat K, Wu X, Deng S, Zhang X, Ho CT. Degradation of 2-Threityl-Thiazolidine-4-carboxylic acid and corresponding browning accelerated by trapping reaction between extra-added xylose and released cysteine during maillard reaction. J Agric Food Chem. 2021;69:10648–56. https://doi.org/10.1021/acs.jafc.1c03727.
38. Huang C, Cui H, Hayat K, Zhang X, Ho CT. Variation of moisture state and taste characteristics during vacuum drying of Maillard reaction intermediates of hydrolyzed soybean protein and characterization of browning precursors via fluorescence spectroscopy. Food Res Int. 2022;162:112086. https://doi.org/10.1016/j.foodres.2022.112086.
39. Sun A, Wu W, Soladoye OP, Aluko RE, Bak KH, Fu Y, Zhang Y. Maillard reaction of food-derived peptides as a potential route to generate meat flavor compounds: a review. Food Res Int. 2022;151:110823. https://doi.org/10.1016/j.foodres.2021.110823.
40. Coleman WM, Perfetti TA. the roles of amino acids and sugars in the production of volatile materials in microwave heated tobacco dust suspensions. Contributions Tob Nicotine Res. 1997;17:75–95. https://doi.org/10.2478/cttr-2013-0660.
41. Arnold M, Gramza-Michałowska A. Enzymatic browning in apple products and its inhibition treatments: a comprehensive review. Compr Rev Food Sci Food Saf. 2022;21:5038–76. https://doi.org/10.1111/1541-4337.13059.

Publisher's Note